Inorganic Chemistry

Article

pubs.acs.org/IC

Reduction of Nitrous Acid with a Macrocyclic Rhodium Complex That Acts As a Functional Model of Nitrite Reductase

Kathleen E. Kristian and Andreja Bakac*

Iowa State University, Ames, Iowa 50011, United States

Supporting Information

ABSTRACT: Nitrous acid reacts with $L^2(H_2O)Rh^{2+}$ (L^2 = *meso*-hexamethylcyclam) in acidic aqueous solutions to generate a strongly absorbing intermediate ***Int-1*** (λ_{max} 400 nm, ε = 1200 M^{-1} cm^{-1}). The reaction follows a mixed second order rate law with $k = (6.9 \pm 0.3) \times 10^4$ M^{-1} s^{-1}, independent of $[H^+]$. The lack of acid dependence shows that ***Int-1*** is a rhodium(II) complex of HNO_2, most reasonably assigned as $L^2(H_2O)Rh(HNO_2)^{2+}$. This species is analogous to the early iron and copper intermediates in the reduction of nitrite by nitrite reductases and by deoxyhemoglobin. In the presence of excess $L^2(H_2O)Rh^{2+}$, the lifetime of ***Int-1*** is about 1 min. It decays to a 1:1 mixture of $L^2(H_2O)RhNO^{2+}$ and $L^2Rh(H_2O)_2^{3+}$ with kinetics that are largely independent of the concentration of excess $L^2(H_2O)Rh^{2+}$ and of $[H^+]$ at $[H^+] < 0.03$ M. At $[H^+] > 0.03$ M, an acid-catalyzed pathway becomes effective, suggesting protonation and dehydration of ***Int-1*** to generate $L^2(H_2O)RhNO^{3+}$ (***Int-2***) followed by rapid reduction of ***Int-2*** by excess $L^2(H_2O)Rh^{2+}$. ***Int-2***, which was generated and characterized independently, is an analog of the electrophilic intermediates in the mechanism of biological reduction of nitrite to •NO. Excess nitrite greatly reduces the lifetime of ***Int-1***, which under such conditions decomposes on a millisecond time scale by nitrite-catalyzed disproportionation to yield $L^2(H_2O)RhNO^{2+}$ and L^2Rh(III). This reaction provides additional support for the designation of ***Int-1*** as a Rh(II) species. The complex reaction mechanism and the detection of ***Int-1*** demonstrate the ability of inorganic complexes to perform the fundamental chemistry believed to take place in the biological reduction of HNO_2 to NO catalyzed by nitrite reductases or deoxyhemoglobin.

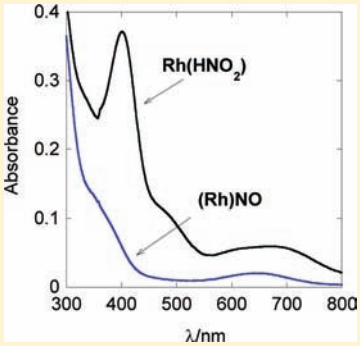

INTRODUCTION

The reduction of nitrous acid is an important reaction in nature and biology where HNO_2/NO_2^- serves as one of the sources of •NO.[1−6] Such reductions are catalyzed by heme or copper nitrite reductases (NiR)[7,8] as well as by deoxyhemoglobin[9] and several other metalloenzymes.[8] NiR-catalyzed reduction is part of the process of denitrification whereby certain bacteria utilize oxo-nitrogen species in place of oxygen as a terminal oxidant in metabolic processes and generate dinitrogen as the final reduced product.[7]

Detailed studies of bacterial NiRs produced evidence of several types of intermediates. A nitrite complex of the fully reduced enzyme Cytochrome *cd1* forms in microseconds[10] and is transformed in the next step to a Fe(II)−NO^+ site. A catalytically competent release of NO was observed at pH 6 but not at pH 7.[11] Electrophilic intermediates generated by protonation and dehydration of coordinated nitrite were observed in other instances as well.[7,12,13] These intermediates dissociate •NO from Fe(III) (or Cu(II)), followed by the reduction of the metal and, in the case of heme NiR, capture of •NO by Fe(II).

Crystal structures are available for the resting state of a Cu−NiR, the nitrite-bound enzyme, and the stable form with NO bound side-on.[12,14] Also, a model of a Cu(I) nitrite complex of NiR, (Pr_3-tacn)$Cu(NO_2)$,[15] was prepared and structurally characterized (Pr = 2-propyl, tacn = tetraazacyclononane). This complex reacts with acids in nonaqueous solvents and generates •NO,[15,16] as does a copper nitrito complex $Cu(Ph_2PC_6H_4(o\text{-}OMe))_2(ONO)$.[17]

At low pH, deoxyhemoglobin and nitrite form Hb(II)-HONO which is converted to a hybridized intermediate $Hb^{(II)}(NO^+) \leftrightarrow Hb^{(III)}NO$ by formal elimination of OH^-. This hybridized intermediate[18,19] is stabilized by interaction with a β-93 thiol group[20,21] that generates a thiyl radical $•SHb^{(II)}NO$ observable by ESR.[19] The equilibrated mixture of $Hb^{(II)}(NO^+) \leftrightarrow Hb^{(III)}NO$ and $•SHb^{(II)}NO$ may provide a pool of bioactive •NO that is not readily captured by $Hb^{(II)}$ or $Hb(O_2)$ and that may be released from red blood cells.[19]

In contrast to these biological systems, abiological reductions of nitrite rarely generate observable intermediates. This is true even for the strongly reducing and highly labile aqua ions of chromium(II) and europium(II), which might be expected to readily capture HNO_2 similar to Cu(I) or Fe(II) centers in NiRs. In the case of chromium, the reaction could lead to an observable $(H_2O)_5CrNO^{3+}$ owing to slow ligand exchange around Cr(III). Instead, the reaction[22] generates $Cr(H_2O)_6^{3+}$ and •NO in a single kinetic step followed by rapid[23] capture of •NO by the second equivalent of $Cr(H_2O)_6^{2+}$. Similarly, Eu(II) reduces HNO_2 to N_2O via •NO and HNO, but no metal-based

Received: March 21, 2012
Published: April 5, 2012

   dx.doi.org/10.1021/ic300597n | *Inorg. Chem.* 2012, 51, 4877−4882

intermediates were observed.[24] Also, polyaminocarboxylate complexes LFe(II) produce $LFe^{II}NO$ without an observable $LFe^{III}NO$.[25]

In search of a potential new route to a macrocyclic rhodium nitrosyl $L^2(H_2O)RhNO^{2+}$, an excellent photochemical source of $^{\bullet}NO$,[26] we explored the reaction of HNO_2 with $L^2(H_2O)Rh^{2+}$ As described below, the desired nitrosyl product is indeed formed, but the reaction involves intermediates that might be more readily associated with biological reductions than with those involving simple inorganic complexes.

EXPERIMENTAL SECTION

Materials. Perchloric acid, trifluoromethane sulfonic (triflic) acid, sodium perchlorate, and lithium perchlorate were obtained from commercial sources at the highest purity available and were used without further purification. Sodium nitrite (99.999%) was obtained from Sigma-Aldrich and used without further purification. Aqueous solutions of sodium nitrite were stored under Ar at their natural pH and always prepared freshly before spectral or kinetic measurements. In-house distilled water was further purified by passage through a Barnstead EASY pure III system.

Solutions of $L^2(H_2O)Rh^{2+}$ were generated by 313 nm photolysis (Luzchem LZC-5 Reactor) of $L^2(H_2O)RhH^{2+}$ under argon.[27] UV–vis spectra and the kinetics of slow reactions were recorded with a Shimadzu 3101 PC spectrophotometer at a constant temperature (25 ± 0.2 °C). An Olis RSM-100 rapid scanning stopped flow spectrophotometer was used for faster kinetics. Kinetic analyses were performed with a KaleidaGraph 4.03 PC software and with Olis GlobalWorks PC software. The detection of free nitrate utilized UV–vis spectroscopy (λ_{max} = 200 nm, ε = 10 000 M^{-1} cm^{-1})[28] after the removal of metal complexes by passage through a column of Sephadex-C25 cation exchange resin. To test for coordinated nitrate, reaction solutions were first allowed to age for the amount of time corresponding to 10 half-lives for nitrate aquation from $L^2(H_2O)Rh(NO_3)^{2+}$.[29] This was followed by ion exchange and UV–vis spectroscopy as described above. $L^2(H_2O)RhNO^{2+}$ was identified and quantified by its characteristic maximum at 650 nm and a shoulder at 390 nm, Figure S1.

Molar Absorptivity of $L^2(H_2O)Rh(HNO_2)^{2+}$ (*Int-1*). This intermediate was generated in a stopped-flow experiment from 0.16 mM $L^2(H_2O)Rh^{2+}$ and 0.05 mM HNO_2 at 0.05 M H^+. Under these conditions, ***Int-1*** forms rapidly (stopped-flow time scale) but decays slowly (minutes). The absorbance increase at 400 nm from five consecutive shots was averaged to give ε_{400} = 1200 M^{-1} cm^{-1}. In another, less accurate experiment, a series of UV–vis spectra were recorded with a conventional spectrophotometer immediately upon adding HNO_2 (final concentration 0.11 mM) to a solution of 0.36 mM $L^2(H_2O)Rh^{2+}$ in 0.01 M $HClO_4$. The value determined from the UV–vis spectrum, 1300 M^{-1} cm^{-1}, is in good agreement with that obtained from the stopped-flow data. The molar absorptivity at 670 nm, $\varepsilon_{670} \approx$ 200 M^{-1} cm^{-1}, was approximated from the absorbance at 670 nm and the value of ε_{400} determined above (1200 M^{-1} cm^{-1}).

Kinetic Measurements. All of the data were obtained at a constant temperature of 25 ± 0.2 °C. Ionic strength and pH were controlled with $HClO_4/NaClO_4$. The kinetics of the decay of ***Int-1*** under conditions of excess $L^2(H_2O)Rh^{2+}$ were determined with a conventional spectrophotometer. The formation of ***Int-1*** under all of the conditions and the decay when HNO_2 was in excess required the use of the stopped flow. The decay rate constant was obtained from the data collected after completion of ≥10 half-lives of the formation step. Olis GlobalWorks software was used to fit the data in the 375–425 nm range. The reported rate constants from these data are the average of at least five values that agree to within 15% or less.

RESULTS

The reaction between HNO_2 and $L^2(H_2O)Rh^{2+}$ in acidic aqueous solutions produces $L^2(H_2O)RhNO^{2+}$ and $L^2Rh^{III}(H_2O)_2^{3+}/L^2(H_2O)Rh^{III}OH^{2+}$ via an intermediate that exhibits maxima at 400 nm (ε = 1200 M^{-1} cm^{-1}) and 670 nm ($\varepsilon \approx$ 200 M^{-1} cm^{-1}), Figure 1. As described in detail below, the

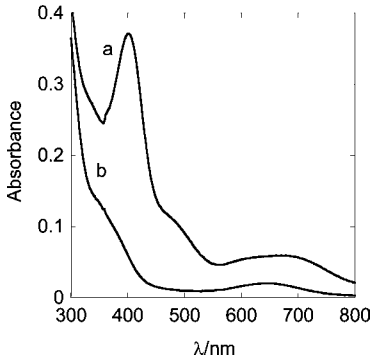

Figure 1. (a) UV–vis spectrum of ***Int-1*** formed in the reaction of $L^2(H_2O)Rh^{2+}$ (0.69 mM) and HNO_2 (0.34 mM) in 0.05 M $HClO_4$. (b) Final spectrum after the decay of ***Int-1*** showing the characteristic 650 nm band of $L^2(H_2O)RhNO^{2+}$.

formation of this intermediate, termed ***Int-1***, obeys mixed second-order kinetics under all of the conditions employed, but the lifetime and rate law for the decomposition of ***Int-1*** to final products change with the concentrations of HNO_2, $L^2(H_2O)Rh^{2+}$, and H^+. Specifically, ***Int-1*** persists for over a minute when $L^2(H_2O)Rh^{2+}$ is in excess but decays in tens of milliseconds when the conditions are reversed so that $[HNO_2] > [L^2(H_2O)Rh^{2+}]$.

Experiments with Excess $L^2(H_2O)Rh^{2+}$. The overall reaction yielded 1 mol of $L^2(H_2O)RhNO^{2+}$ per mole of HNO_2 as in eq 1. The other rhodium product is shown as $L^2(H_2O)RhOH^{2+}$, although it is probably a mixture of $L^2(H_2O)RhOH^{2+}$ and $L^2Rh(H_2O)_2^{3+}$ assuming that the K_a for $L^2Rh(H_2O)_2^{3+}$ is similar to that for the closely related $L^1Rh(H_2O)_2^{3+}$ (L^1 = cyclam), K_a = 0.0031 M.[30]

$$2L^2(H_2O)Rh^{2+} + HNO_2 \rightarrow L^2(H_2O)RhNO^{2+} + L^2(H_2O)RhOH^{2+} \quad (1)$$

In the presence of a large excess of $L^2(H_2O)Rh^{2+}$, the kinetic traces for the formation of ***Int-1***, eq 2, were exponential and yielded pseudo-first-order rate constants that exhibited linear dependence on the concentration of $L^2(H_2O)Rh^{2+}$, as shown in Figure 2. These results establish the mixed second order rate law of eq 3, where $k_1 = (6.9 \pm 0.3) \times 10^4$ M^{-1} s^{-1}, independent of ionic strength and acid concentration in the range 0.010–0.25 M.

$$L^2(H_2O)Rh^{2+} + HNO_2 \rightarrow L^2(H_2O)Rh^{II}(HNO_2)^{2+} (\equiv \textbf{\textit{Int-1}}) \quad (2)$$

$$\text{rate} = k_1[L^2(H_2O)Rh^{2+}][HNO_2] \quad (3)$$

The decay of ***Int-1*** followed exponential kinetics with rate constants exhibiting only slight dependence on $[L^2(H_2O)Rh^{2+}]$, $k = (8.6 \pm 0.6) \times 10^{-3} + (4.7 \pm 0.8)$ $[L^2(H_2O)Rh^{2+}]$, and no dependence on acid concentration in the range 0.005 M ≤ $[H^+]$ ≤ 0.030 M, Figures 3 and 4. An H^+-assisted pathway sets in at higher $[H^+]$, Figure 4.

Experiments with Excess HNO_2. The reaction again yielded 0.5 equivalents of $L^2(H_2O)RhNO^{2+}$ per mole of $L^2(H_2O)Rh^{2+}$ as in eq 1. No nitrate, free or bound to $L^2Rh(III)$, was detected under any conditions. The other

dx.doi.org/10.1021/ic300597n | Inorg. Chem. 2012, 51, 4877–4882

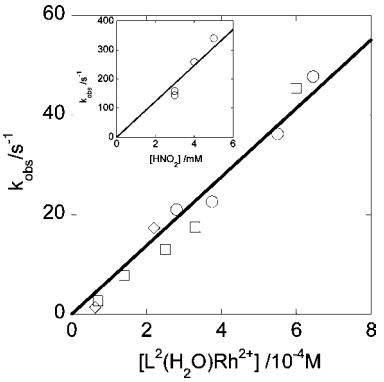

Figure 2. Plot of k_{obs}/s^{-1} vs $[L^2(H_2O)Rh^{2+}]$ for the formation of ***Int-1*** from $L^2(H_2O)Rh^{2+}$ and HNO_2 (0.01 mM) in 0.01 M $HClO_4$ (squares), 0.01 M CF_3SO_3H (circles), and 0.25 M CF_3SO_3H (diamonds). Inset: plot of k_{obs}/s^{-1} vs $[HNO_2]$ for experiments with limiting $[L^2(H_2O)Rh^{2+}]$ (0.15−0.30 mM) in 0.050 M $HClO_4$.

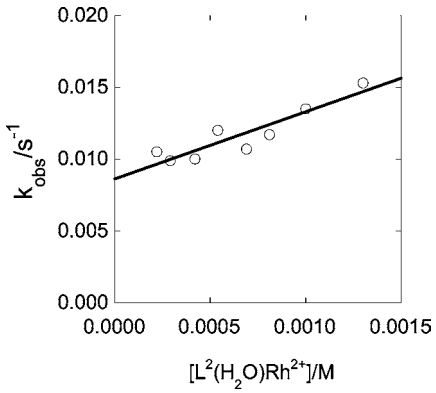

Figure 3. Plot of k_{obs}/s^{-1} vs $[L^2(H_2O)Rh^{2+}]$ for the decay of ***Int-1*** generated from $L^2(H_2O)Rh^{2+}$ and HNO_2 (0.02 mM) in 0.05 M $HClO_4$.

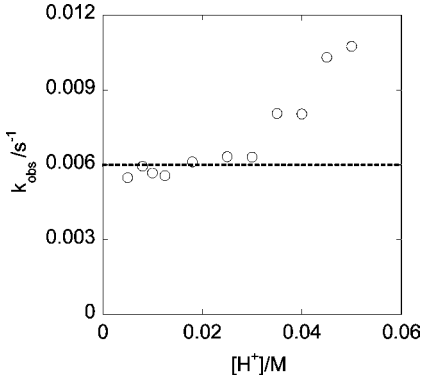

Figure 4. Plot of k_{obs}/s^{-1} vs $[H^+]$ for the decay of ***Int-1*** generated from $L^2(H_2O)Rh^{2+}$ (0.4 mM) and HNO_2 (0.02 mM) at 0.06 M ionic strentgth.

Rh(III) product was deduced to be mostly or exclusively $L^2Rh(H_2O)_2^{3+}/L^2(H_2O)Rh(OH)^{2+}$ based on experiments that used only a small (2−3 fold) excess of HNO_2. These conditions made it possible to estimate the amount of unreacted HNO_2 from its characteristic UV spectrum after correction for the contribution from $L^2(H_2O)RhNO^{2+}$ (ε_{383} = 62 $M^{-1}cm^{-1}$). The data were consistent with the overall stoichiometry shown in eq 1 and provided no evidence for measurable amounts of nitrite coordinated to Rh(III).

Owing to the rapid, second-order disappearance of ***Int-1*** in the presence of excess HNO_2, the formation step was not fully separated from the decay. The rate constant for the formation step was therefore determined from initial rates in stopped flow experiments using 3−5 mM HNO_2 and 0.15−0.30 mM $L^2(H_2O)Rh^{2+}$ in 0.050 M $HClO_4$. The initial rates were divided by the concentration of $L^2(H_2O)Rh^{2+}$ and the resulting pseudo-first-order rate constants plotted against $[HNO_2]$ in the inset in Figure 2. The value of the rate constant obtained from the slope, $k_1 = (6.2 \pm 0.4) \times 10^4$ M^{-1} s^{-1}, is in good agreement with the result obtained under reverse concentration conditions in the main plot in Figure 2 and confirms the 1:1 kinetic stoichiometry.

The disappearance of ***Int-1*** obeyed second-order kinetics, as illustrated in Figure 5. The data were fitted to the expression in

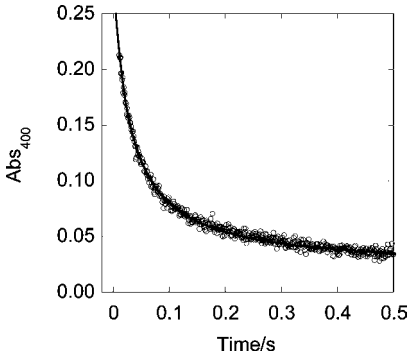

Figure 5. Kinetic trace and a fit according to eq 4 for the decay of ***Int-1*** formed in the reaction between $L^2(H_2O)Rh^{2+}$ (0.3 mM) and HNO_2 (10 mM) in 0.04 M $HClO_4$. The formation of ***Int-1*** (data not shown) is complete in ca. 10 ms under these conditions.

eq 4 and yielded the rate constant k_5 that exhibits first-order dependence on $[HNO_2]$ and inverse first-order dependence on $[H^+]$ (Figure 6), leading to the overall rate law in eq 5, where k_5

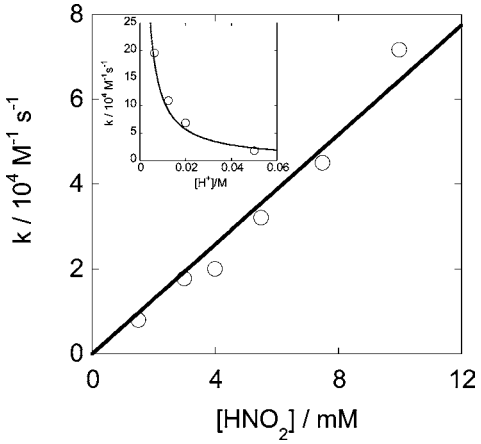

Figure 6. Dependence of the second-order rate constant for decay of ***Int-1*** on $[HNO_2]$ (at $[H^+]$ = 0.050 M, main figure) and on $[H^+]$ (at $[HNO_2]$ = 3.0 mM, inset).

= $(3.2 \pm 0.2) \times 10^5$ M^{-1} s^{-1}. This behavior persisted even with ≤2 fold excess of HNO_2, which supports our earlier conclusion that significant amounts of nitrite were not retained in the Rh(III) product because in that case the nitrite-catalyzed path would cease to operate before the reaction is complete.

dx.doi.org/10.1021/ic300597n | *Inorg. Chem.* 2012, 51, 4877−4882

$$Abs_t = Abs_\infty + \frac{Abs_0 - Abs_\infty}{1 + 2k[\textbf{\textit{Int-1}}]_0 t} \quad (4)$$

$$d[\textbf{\textit{Int-1}}]/dt = k_S[\textbf{\textit{Int-1}}]^2[HNO_2][H^+]^{-1} \quad (5)$$

DISCUSSION

Nature of Int-1. The mixed second-order rate law for the formation of ***Int-1*** shows the composition of the transition state is $[L^2(H_2O)Rh^{2+}, HNO_2, \pm nH_2O]^{\ddagger}$. Importantly, no protons are consumed or liberated, which rules out the nitrite anion as a reactant. The evidence presented so far and discussed in more detail below leads us to conclude that the composition of ***Int-1*** is quite similar to that of the transition state for its formation, i.e., that no rapid acid/base chemistry takes place after the rate determining step. Reaction 2 goes to completion under all of the conditions examined as judged by the constancy of ε_{400} and by the lack of an intercept in k_{obs} versus concentration plot in Figure 2. These data place a lower limit for the apparent equilibrium constant K_2 at $\geq 10^6$ M^{-1}, a value much greater than would be expected for simple ligation of a neutral monodentate species to a low-spin d^7 metal center. The large K_2 and the strong new absorption features in the UV−vis provide evidence for charge-transfer interactions in ***Int-1*** that are not present in the reactants.

Attempts to further characterize ***Int-1*** by IR spectroscopy were thwarted by weak signals in aqueous solutions. Nonetheless, some possibilities can be eliminated. Specifically, the long lifetime of ***Int-1*** in the presence of excess $L^2(H_2O)Rh^{2+}$ shows that ***Int-1*** is distinctly different from $L^2(H_2O)RhNO^{3+}$, an analog of the strongly electrophilic intermediates generated by NiRs. We have shown previously[27] that $L^2(H_2O)RhNO^{3+}$ is a powerful oxidant (E^0 = 1.31 V vs NHE) that reacts rapidly even with poor reductants such as $Ru(bpy)_3^{2+}$, (E^0 = 1.26 V, $k = 1.5 \times 10^6$ M^{-1} s^{-1}). The reduction by $L^2(H_2O)Rh^{2+}$ (E^0 = 0.13 V)[31] should be at least as fast and probably much faster, but the disappearance of ***Int-1*** in the presence of $L^2(H_2O)Rh^{2+}$ takes minutes and the main path is independent of the concentration of $L^2(H_2O)Rh^{2+}$, Figure 3.

$L^2(H_2O)RhNO^{3+}$ is, however, believed to be involved in the overall reaction, but at a later stage, namely as an intermediate in the decay of ***Int-1***. In this scenario, coordinated HNO_2 in ***Int-1*** is cleaved in a heterolytic process to generate $L^2(H_2O)RhNO^{3+}$ or its conjugate base $L^2(HO)RhNO^{2+}$, followed by the reduction with $L^2(H_2O)Rh^{2+}$, eqs 6−8 and Scheme 1. This mechanism accounts for the first-order kinetics of the major path for the decay of ***Int-1*** in Figure 3, correctly leads to the observed overall stoichiometry in eq 1, and requires that the reduction of $L^2(H_2O)RhNO^{3+}$ by $L^2(H_2O)Rh^{2+}$ be fast, in agreement with our expectations outlined above.

$$L^2(H_2O)Rh^{II}(HNO_2)^{2+} (\equiv \textbf{\textit{Int-1}}) \rightarrow L^2(HO)RhNO^{2+} + H_2O \quad (6)$$

$$L^2(HO)RhNO^{2+} + H^+ \rightleftarrows L^2(H_2O)RhNO^{3+} \quad (7)$$

$$L^2(H_2O)RhNO^{3+} + L^2(H_2O)Rh^{2+} + H_2O \xrightarrow{fast} L^2(H_2O)Rh(NO)^{2+} + L^2(H_2O)_2Rh^{3+} \quad (8)$$

Another mechanism consistent with experimental observations is based on homolytic cleavage of ***Int-1*** to generate $L^2(H_2O)RhOH^{2+}$ and free $^{\bullet}NO$, much like the proposed reduction of HNO_2 by other transition metal complexes.[22,24,25]

Scheme 1

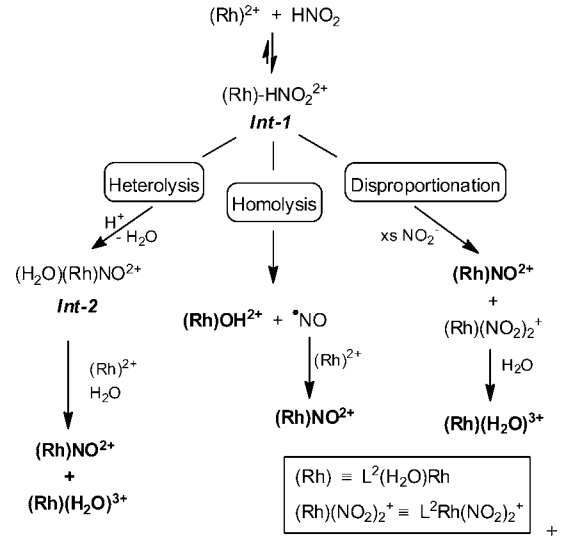

In the next step, $^{\bullet}NO$ rapidly couples with the second equivalent of $L^2(H_2O)Rh^{2+}$ to form $L^2(H_2O)RhNO^{2+}$, eqs 9 and 10 and Scheme 1.

$$L^2(H_2O)Rh^{II}(HNO_2)^{2+} \rightarrow L^2(H_2O)Rh(OH)^{2+} + {}^{\bullet}NO \quad (9)$$

$$L^2(H_2O)Rh^{2+} + {}^{\bullet}NO \rightarrow L^2(H_2O)Rh(NO)^{2+} \quad (10)$$

The two mechanisms result in the same stoichiometry (eq 1) and are kinetically indistinguishable, but the operation of a $[H^+]$-assisted pathway (Figure 4) favors the heterolytic process in eqs 6−8. The attack of H^+ at coordinated HNO_2 would facilitate electron transfer and dehydration, similar to the H^+-assisted formation of NO^+ from free HNO_2.[32] Corresponding reactions of enzymes and their models are also promoted by H^+,[13,18] but in those cases nitrite is initially present as NO_2^-. ***Int-1***, on the other hand, contains HNO_2, which does not require external H^+ but a new mechanistic path that utilizes an additional equivalent of H^+ is enabled at higher acidity ($\geq$0.03 M). It is less likely that the homolytic cleavage of coordinated HNO_2 in eq 9 would be subject to acid catalysis, although this possibility cannot be completely ruled out.

A parallel path from ***Int-1*** to products involves a bimolecular reaction with $L^2(H_2O)Rh^{2+}$, as indicated by the slope of the line in Figure 3. This reaction is significant only at high concentrations of $L^2(H_2O)Rh^{2+}$. The small rate constant, 4.6 M^{-1} s^{-1}, is consistent with both an outer-sphere process and an inner-sphere reaction between the sterically encumbered L^2 complexes.[33]

Nitrite-Catalyzed Decay of Int-1. The rate law in eq 5 for the decay of ***Int-1*** under conditions of excess HNO_2 is most reasonably interpreted as disproportionation of ***Int-1*** catalyzed by NO_2^- as in eq 11 and 12. Strong σ donor ligands, such as halides, and strong π acceptors, such as CO, are known to facilitate disproportionation of Rh(II) complexes.[34,35] In the course of this study, we have also observed rapid disproportionation of $L^2(H_2O)Rh^{2+}$ in the presence of chloride ions to give a 1:1 mixture of $L^2(H_2O)RhH^{2+}$ and $L^2RhCl_2^+$.[36] In the absence of coordinating anions, $L^2(H_2O)Rh^{2+}$ is stable for long periods of time. Similarly, bound HNO_2 in ***Int-1*** does not induce disproportionation, but the lack of an inverse $[H^+]$ path

dx.doi.org/10.1021/ic300597n | Inorg. Chem. 2012, 51, 4877−4882

that does not require external HNO_2/NO_2^- under the conditions in Figure 4 ($[H^+] \geq 5$ mM) is surprising.

$$2L^2Rh(HNO_2)^{2+}(\equiv \textit{Int-1}) \xrightarrow{NO_2^-} L^2Rh^{III}(NO_2)_2^+ + L^2Rh^{I}(HNO_2)^+ + H^+ \quad (11)$$

$$L^2Rh^{I}(HNO_2)^+ + H^+ \xrightarrow{fast} L^2(H_2O)RhNO^{2+} \quad (12)$$

On the basis of the rate law and products, the disproportionation is suggested to involve a transition state or intermediate that has the additional NO_2^- coordinated to one of the rhodium partners followed by either outer-sphere or nitrite-bridged electron transfer. In view of the large reaction rates despite steric crowding at rhodium, we prefer an outer-sphere process. Precedents exist for fast outer-sphere reactions of metal complexes containing saturated N_4 macrocycles.[37,38]

In either case, $L^2Rh^{III}(NO_2)_2^+$ and $L^2Rh^{I}(HNO_2)^+$ are produced followed by immediate H^+-assisted intramolecular electron transfer in the latter to generate $L^2(H_2O)RhNO^{2+}$. This step explains why nitrite-induced disproportionation does not generate $L^2(H_2O)RhH^{2+}$, which would be expected from a reaction between free Rh(I) and H^+.[36] Alternatively, the disproportionation may be a concerted process that bypasses $L^2Rh^{I}(HNO_2)^+$ as a discrete intermediate and yields $L^2Rh^{III}(NO_2)_2^+$ and $L^2(H_2O)RhNO^{2+}$ directly.

Spectral analysis and kinetic data under conditions of limiting excess of HNO_2 showed that nitrite is not coordinated to Rh(III) in the final product. Thus, rapid dissociation of nitrite had to take place either as part of the disproportionation process or from the initially formed $L^2Rh^{III}(NO_2)_2^+$. However, nitro complexes of Rh(III), including $L^2(H_2O)RhNO_2^{2+}$,[30] $L^1(H_2O)RhNO_2^{2+}$ (L^1 = cyclam),[39] and $(NH_3)_5Rh(NO_2)^{2+}$, dissociate nitrite only very slowly in acidic solutions.[40] The nitrito complex, $(NH_3)_5Rh(ONO)^{2+}$, on the other hand, readily undergoes acid-catalyzed aquation. The reaction in 0.1 M acid is complete in several minutes at room temperature.[40] These data suggest that ***Int-1*** and products derived from it may have HNO_2 bound via oxygen, which would result in rapid aquation of the initially formed Rh(III) product(s). It is reasonable to expect for axial sites in a sterically crowded macrocyclic complex to be more labile than the single site in the pentaammine nitrito complex. Recent calculations[9] provided some support for the feasibility of HNO_2 coordination via oxygen in the reaction of deoxyhemoglobin with nitrite.

In the mechanistic sense, the disproportionation provides additional strong support for the assignment of ***Int-1*** as a Rh(II) complex. The decay of intermediates in the $Hb^{(II)}$–nitrite reaction is also accelerated by nitrite, but in that case the effect was attributed to conformational changes that facilitate the transfer of $^{\bullet}NO$ or NO^+ to β-93 thiol.[41]

CONCLUSIONS

Intermediates such as ***Int-1*** are highly unusual for reductions of nitrous acid by transition metal complexes in aqueous solution. In terms of oxidation states and the extent of protonation, ***Int-1*** is closely related to the first intermediate generated in the complex reaction of HNO_2 with deoxyhemoglobin, i.e., $Hb^{(II)}$–(HNO_2), which is believed to be stabilized by conformational changes in the ligand pocket.[18] It is highly unlikely that significant conformational changes are involved in stabilizing ***Int-1*** given that L^2 is a small, saturated macrocyclic ligand. Stabilizing charge-transfer interactions are however evidenced by the strong features in the UV–vis spectrum.

The rarity of species such as ***Int-1*** is associated, in part, with unfavorable kinetic parameters, i.e., slow formation and/or fast decay, which would make the detection difficult. To the best of our knowledge, ***Int-1*** is the first nonbiological intermediate of this type observed in aqueous solution. Examples in other solvents are also extremely rare.[16] The critical role of kinetics was demonstrated recently in the case of $(Pr_3\text{-tacn})Cu^{I}(NO_2)$, which decomposes slowly in CH_2Cl_2 at 233 K by the addition of acetic acid and generates $^{\bullet}NO$ and a stable Cu(II) product without observable intermediates.[16] A much stronger acid, CF_3COOH, on the other hand, quickly protonates the coordinated nitrite to generate $(Pr_3\text{-tacn})Cu^{I}(NO_2HOCOCF_3)$, which was detected at 203 K.[16] The protonated species exhibits strong transitions in the UV–vis that diminish upon intramolecular electron transfer that eventually leads to Cu(II) and $^{\bullet}NO$.

The combination of rapid binding of HNO_2 to $L^2(H_2O)Rh^{2+}$ in this work and relatively slow decay of ***Int-1*** made it possible to observe and identify this intermediate and to illustrate the ability of simple inorganic complexes to carry out the fundamental chemistry believed to take place in the complex biological reduction of HNO_2 to NO catalyzed by NiRs or deoxyhemoglobin. The formation of intermediates that are analogous to, but more persistent than those generated in biological reactions should enable detailed chemical and spectroscopic studies and provide important clues about the complex chemistry of metalloenzymes.

ASSOCIATED CONTENT

Supporting Information

UV–vis spectra of $L^2Rh(H_2O)_2^{3+}$, $L^2(H_2O)RhNO^{2+}$, and HNO_2 (Figure S1). This material is available free of charge via the Internet at http://pubs.acs.org.

AUTHOR INFORMATION

Corresponding Author

*E-mail: bakac@iastate.edu.

Notes

The authors declare no competing financial interest.

ACKNOWLEDGMENTS

We are grateful to Dr. Wenjing Song for assistance with preliminary experiments, and to Dr. Pestovsky for useful discussions. This work was supported by a grant from the National Science Foundation, CHE 0602183. Some of the work was conducted with the use of facilities at the Ames Laboratory.

REFERENCES

(1) Bryan, N. S. *Free Radical Biol. Med.* **2006**, *41*, 691–701.
(2) Gladwin, M. T.; Schechter, A. N.; Kim-Shapiro, D. B.; Patel, R. P.; Hogg, N.; Shiva, S.; Cannon, R. O.; Kelm, M.; Wink, D. A.; Espey, M. G.; Oldfield, E. H.; Pluta, R. M.; Freeman, B. A.; Lancaster, J. R.; Feelisch, M.; Lundberg, J. O. *Nature Chem. Biol.* **2005**, *1*, 308–314.
(3) Gladwin, M. T.; Raat, N. J. H.; Shiva, S.; Dezfulian, C.; Hogg, N.; Kim-Shapiro, D. B.; Patel, R. P. *Am. J. Physiol.* **2006**, *291*, H2026–H2035.
(4) Kevil, C. G.; Kolluru, G. K.; Pattillo, C. B.; Giordano, T. *Free Radical Biol. Med.* **2011**, *51*, 576–593.
(5) Lundberg, J. O.; Weitzberg, E.; Gladwin, M. T. *Nat. Rev. Drug Discovery* **2008**, *7*, 156–167.

(6) Sturms, R.; DiSpirito, A. A.; Hargrove, M. S. *Biochemistry* **2011**, *50*, 3873−3878.
(7) Averill, B. A. In *Biological Inorganic Chemistry. Structure and Reactivity*; Bertini, I., Gray, H. B., Stiefel, E. I., Valentine, J. S., Eds.; University Science Books: Sausalito, CA, 2007; pp 494−507.
(8) Schopfer, M. P.; Wang, J.; Karlin, K. D. *Inorg. Chem.* **2010**, *49*, 6267−6282.
(9) Perissinotti, L. L.; Marti, M. A.; Doctorovich, F.; Luque, F. J.; Estrin, D. A. *Biochemistry* **2008**, *47*, 9793−9802.
(10) Sam, K. A.; Strampraad, M. J. F.; De Vries, S.; Ferguson, S. J. *J. Biol. Chem.* **2008**, *283*, 27403−27409.
(11) Sam, K. A.; Tolland, J. D.; Fairhurst, S. A.; Higham, C. W.; Lowe, D. J.; Thorneley, R. N. F.; Allen, J. W. A.; Ferguson, S. J. *Biochem. Biophys. Res. Commun.* **2008**, *371*, 719−723.
(12) Antonyuk, S. V.; Strange, R. W.; Sawers, G.; Eady, R. R.; Hasnain, S. S. *Proc. Natl. Acad. Sci. U. S. A.* **2005**, *102*, 12041−12046.
(13) Wasser, I. M.; de Vries, S.; Moeenne-Locoz, P.; Schroeder, I.; Karlin, K. D. *Chem. Rev.* **2002**, *102*, 1201−1234.
(14) Tocheva, E. I.; Resell, F.; Mauk, A. G.; Murphy, M. E. P. *Science* **2004**, *304*, 867−870.
(15) Halfen, J. A.; Mahapatra, S.; Wilkinson, E. C.; Gengenbach, A. J.; Young, V. G. J.; Que, L. J.; Tolman, W. B. *J. Am. Chem. Soc.* **1996**, 118.
(16) Kujime, M.; Fuji, H. *Angew. Chem., Int. Ed.* **2006**, *45*, 1089−1092.
(17) Chuang, W.-J.; Lin, I.-J.; Chen, H.-Y.; Chang, Y.-L.; Hsu, S. C. N. *Inorg. Chem.* **2010**, *49*, 5377−5384.
(18) Salgado, M. T.; Nagababu, E.; Rifkind, J. M. *J. Biol. Chem.* **2009**, *284*, 12710−12718.
(19) Salgado, M. T.; Ramasamy, S.; Tsuneshige, A.; Manoharan, P. T.; Rifkind, J. M. *J. Am. Chem. Soc.* **2011**, *133*, 13010−13022.
(20) Jia, L.; Bonaventura, C.; Bonaventura, J.; Stamler, J. S. *Nature (London)* **1996**, *380*, 221−226.
(21) Pawloski, J. R.; Hess, D. T.; Stamler, J. S. *Nature* **2001**, *409*, 622−626.
(22) Ogino, H.; Tsukahara, K.; Tanaka, N. *Bull. Chem. Soc. Jpn.* **1974**, *47*, 308−311.
(23) Nemes, A.; Pestovsky, O.; Bakac, A. *J. Am. Chem. Soc.* **2002**, *124*, 421−427.
(24) Fraser, R. T. M.; Lee, R. N.; Hayden, K. *J. Chem. Soc. A* **1967**, 741−746.
(25) Zang, V.; Van Eldik, R. *Inorg. Chem.* **1990**, *29*, 4462−4468.
(26) Song, W.; Kristian, K.; Bakac, A. *Chem.—Eur. J.* **2011**, *17*, 4513−4517.
(27) Kristian, K.; Song, W.; Ellern, A.; Guzei, I. A.; Bakac, A. *Inorg. Chem.* **2010**, *49*, 7182−7187.
(28) Endicott, J. F. In *Concepts of Inorganic Photochemistry*; Adamson, A. W., Fleischauer, P. D., Eds.; Wiley: New York, 1975; Chapter 3.
(29) Pestovsky, O.; Bakac, A. *J. Am. Chem. Soc.* **2002**, *124*, 1698−1703.
(30) Szajna-Fuller, E.; Bakac, A. *Dalton Trans.* **2011**, *40*, 10598−10602.
(31) Furczon, M.; Pestovsky, O.; Bakac, A. *Inorg. Chem.* **2007**, *46*, 11461−11466.
(32) Benton, D. J.; Moore, P. *J. Chem. Soc. A* **1970**, 3179−3182.
(33) Bakac, A. *J. Am. Chem. Soc.* **1997**, *119*, 10726−10731.
(34) DeWit, D. G. *Coord. Chem. Rev.* **1996**, *147*, 209−246.
(35) Feller, M.; Ben-Ari, E.; Gupta, T.; Shimon, L. J. W.; Leitus, G.; Diskin-Posner, Y.; Weiner, L.; Milstein, D. *Inorg. Chem.* **2007**, *46*, 10479−10490.
(36) Bakac, A.; Kristian, K. Work in progress.
(37) Liteplo, M. P.; Endicott, J. F. *Inorg. Chem.* **1971**, *10*, 1420−1430.
(38) Bakac, A.; Espenson, J. H. *J. Phys. Chem.* **1993**, *97*, 12249−12253.
(39) Bounsall, E. J.; Koprich, S. R. *Can. J. Chem.* **1970**, *48*, 1481−1491.
(40) Crossland, B. E.; Staples, P. J. *J. Chem. Soc. A* **1971**, 2853−2856.
(41) Nagababu, E.; Ramasamy, S.; Rifkind, J. M. *Biochemistry* **2007**, *46*, 11650−11659.